440-kD Ankyrin$_B$: Structure of the Major Developmentally Regulated Domain and Selective Localization in Unmyelinated Axons

Wing Chan,* Ekaterini Kordeli,‡ and Vann Bennett‡

*Howard Hughes Medical Institute and Departments of Cell Biology and ‡Biochemistry, Duke University Medical Center, Durham, North Carolina 27710

Abstract. 440-kD ankyrin$_B$ is an alternatively spliced variant of 220-kD ankyrin$_B$, with a predicted 220-kD sequence inserted between the membrane/spectrin binding domains and COOH-terminal domain (Kunimoto, M., E. Otto, and V. Bennett. 1991. *J. Cell Biol.* 236:1372-1379). This paper presents the sequence of 2085 amino acids comprising the alternatively spliced portion of 440-kD ankyrin$_B$, and provides evidence that much of the inserted sequence has the configuration of an extended random coil. Notable features of the inserted sequence include a hydrophilicity profile that contains few hydrophobic regions, and 220 predicted sites for phosphorylation by protein kinases (casein kinase 2, protein kinase C, and proline-directed protein kinase). Secondary structure and folding of the inserted amino acid residues were deduced from properties of recombinant polypeptides. Frictional ratios of 1.9-2.4 were calculated from Stokes radii and sedimentation coefficients, for polypeptides comprising 70% of the inserted sequence, indicating a highly asymmetric shape. Circular dichroism spectra of these polypeptides indicate a nonglobular structure with negligible α-helix or β sheet folding. These results suggest a ball-and-chain model for 440-kD ankyrin$_B$ with a membrane-associated globular head domain and an extended filamentous tail domain encoded by the inserted sequence. Immunofluorescence and immunoblot studies of developing neonatal rat optic nerve indicate that 440-kD ankyrin$_B$ is selectively targeted to premyelinated axons, and that 440-kD ankyrin$_B$ disappears from these axons coincident with myelination. Hypomyelinated nerve tracts of the myelin-deficient *Shiverer* mice exhibit elevated levels of 440-kD ankyrin$_B$. 440-kD ankyrin$_B$ thus is a specific component of unmyelinated axons and expression of 440-kD ankyrin$_B$ may be downregulated as a consequence of myelination.

ANKYRINS are a family of spectrin-binding proteins that link the spectrin/actin network to cytoplasmic domains of integral proteins that include ion channels and cell adhesion molecules (Bennett, 1992; Bennett and Gilligan, 1993; Davis et al., 1993). Ankyrins contain three structural domains: (*a*) an NH$_2$-terminal 89-95-kD membrane-binding domain (Davis and Bennett, 1990*a*); (*b*) a 62-kD domain that binds to spectrin (Bennett, 1978); and (*c*) a COOH-terminal domain that is the target of alternative splicing and represents the most variable domain among different ankyrins. A striking feature of the membrane-binding domain is the presence of 24 tandem repeats of 33 amino acids. The 33-residue repeats are necessary and sufficient for association of ankyrin with the anion exchanger (Davis and Bennett, 1990*b*; Davis et al., 1991), the voltage-dependent sodium channel (Srinivasan et al., 1992), and nervous system cell adhesion molecules related to L1 and neurofascin (Davis et al., 1993).

Three different ankyrins are currently known to be expressed in brain tissue: (*a*) ankyrin$_R$, which is also expressed in erythrocytes; (*b*) ankyrin$_B$, which is the major ankyrin in brain and has at least two alternatively spliced products; and (*c*) ankyrin$_{node}$, which is localized in axonal initial segments and nodes of Ranvier of myelinated axons (Kordeli and Bennett, 1991; Kordeli et al., 1990). Ankyrin$_B$ includes two isoforms of 220 and 440 kD which are products of alternatively spliced pre-mRNAs encoded by a single gene (Otto et al., 1991). 220-kD ankyrin$_B$ is the major ankyrin isoform in adult brain (Kordeli and Bennett, 1991; Kordeli et al., 1990). 440-kD ankyrin$_B$ (The estimate of 440 kD is based on the mobility on SDS-PAGE. The actual MW would be 431 kD based on cDNA sequence, assuming no additional alternate splicing of the pre-mRNA.), in contrast, is maximally expressed in developing neonatal rat brain, with a peak at postnatal day 10 which decreases to ∼30% of the maximal level in adult brain (Kunimoto et al., 1991). 440-kD ankyrin$_B$ is most abundant in regions comprised primarily of axons and dendrites of neurons (Kunimoto et al., 1991).

440-kD ankyrin$_B$ shares the same NH$_2$-terminal and
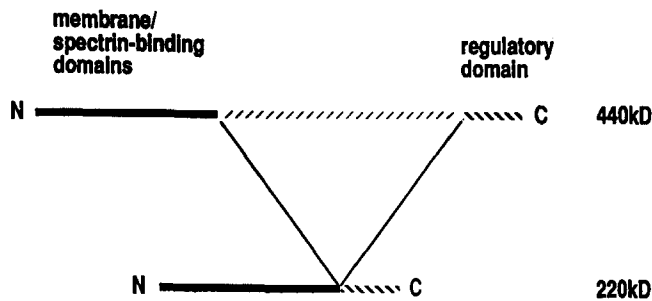
Figure 1. Schematic representation of the alternatively spliced products of brain ankyrin. The 220-kD ankyrin_B (actual molecular mass = 208 kD) is the major isoform in adult rat brain tissue. 440-kD ankyrin_B (actual molecular mass = 431 kD) is preferentially expressed in neonatal brain.

COOH-terminal domains as 220-kD ankyrin_B (Kunimoto et al., 1991; Otto et al., 1991). However, 440-kD ankyrin_B contains, in addition, an inserted domain estimated to be 220 kD located between the membrane/spectrin binding domains and the COOH-terminal domain (Fig. 1). In this paper, we report the amino acid sequence of the inserted region of the 440-kD ankyrin_B (actual molecular mass = 228 kD), and present evidence that a major portion of the inserted domain is folded as an extended, random coil. Studies with neonatal rat optic nerve and the hypomyelinating mutant *Shiverer* mouse demonstrate that 440-kD ankyrin_B is targeted to premyelinated axons, and disappears coincident with my-elination.

Materials and Methods

Materials

Carrier-free Na^{125}I, (α-^{32}P)dCTP, and multiprime DNA labeling system were from Amersham Corp. (Arlington Heights, IL). Bolton-Hunter reagent labeled with ^{125}I was from ICN Biomedicals, Inc. (Costa Mesa, CA). Human brain stem lambda gt11 library was graciously provided by Dr. C. Luts-Freymuth and Dr. J. Keene (Department of Microbiology, Duke University, Durham, NC). pGEM4Z and pGEMEX DNA vectors were from Promega (Madison, WI). Restriction enzymes and DNA ligase were from New-England Biolabs (Beverly, MA), IBI (New Haven, CT), and Promega. Oligonucleotides were synthesized from the Howard Hughes Medical Institute Biopolymers Facility. Nylon membranes for library screening were from DuPont-NEN, Boston, MA. Sodium phosphate (monobasic and dibasic), EDTA, sodium azide, Tween-20, leupeptin, pepstatin, benzamidine, phenylmethylsulphonyl fluoride, and ampicillin were from Sigma Chemical Co. (St. Louis, MO). Sucrose was from Schwarz/Mann. Protein A, isopropyl β-D-thiogalactopyranoside, Superose 12, 6, and cyanogen bromide-activated CL-4B sepharose were from Pharmacia LKB Biotechnology Inc. (Piscataway, NJ). DNAase I was from U.S. Biochemical Corp. (Cleveland, OH). Anti-myelin basic protein mouse monoclonal antibody was from Boehringer Mannheim (Indianapolis, IN). Unconjugated rabbit anti-mouse IgG was from Pierce (Rockford, IL).

cDNA Characterization

Two previously isolated cDNA clones were used as probes to obtain cDNA clones for the 440 ankyrin_B from a fetal human brain stem library. Hybridization was performed at 42°C overnight and filters were washed at 2× SSC at 65°C, followed by 0.1× SSC at room temperature. Positive clones were subsequently subcloned into pGEM4Z plasmid vector and sequenced in both directions by the dideoxy-chain termination method (Sambrook et al., 1989).

Expression of cDNA Clones in E. coli and Purification of Recombinant Polypeptides

cDNA clones (λ110, λ502, and λ606) were amplified by the polymerase chain reaction. The primers used in the PCR reactions contained NheI restriction site at the 5' end and XhoI restriction site and a stop codon at the 3' end. The amplified DNA was digested with NheI and XhoI and then subcloned into pGEMEX expression vector. Plasmids containing inserts were electroporated into the BL21pLysS bacterial strain.

One liter of bacterial cultures were grown to A$_{650}$ = 0.3 and induced with 0.5 mM isopropyl β-D-thiogalactopyranoside for 1.5–2 h. Cultures were centrifuged at 5,000 rpm for 10 min, and the resulting bacterial pellets was washed with 150 mM NaCl, 10 mM sodium phosphate, pH 7.4, and resuspended in 50 mM sodium phosphate, 1 mM NaEDTA, 25% sucrose, pH 8.2. The cells were lysed with 1 mg/ml lysozyme on ice for 30 min in the presence of the following protease inhibitors: 10 μg/ml leupeptin, 10 μg/ml pepstatin, 5 mM benzamidine, 50 μg/ml phenylmethylsulphonyl fluoride and 0.01% diisopropyl fluorophosphate. MgCl$_2$ and DNase I were added to the suspension to give a final concentration of 10 mM and 40 μg/ml, respectively, and incubations continued on ice for 15 min. Two volumes of lysis buffer (20 mM sodium phosphate, 0.2 M NaCl, 2 mM NaEDTA, 1 mM NaN$_3$, 1% Triton X-100, and 1 mM DTT) were added and the suspension passed through a 20-gauge needle three times and centrifuged at 5000 rpm for 20 min. The supernatant was pooled and ammonium sulfate was added to a final concentration of 60%. The precipitate was resuspended in Superose 6 column buffer (1 M NaBr, 10 mM sodium phosphate, 1 mM NaEDTA, 1 mM NaN$_3$, and 0.05% Tween-20). The suspension was dialyzed against the column buffer containing 10% sucrose. Undissolved material was removed by centrifugation at 14,000 rpm for 30 min and the supernatant was loaded onto Superose 6 or Superose 12 gel filtration columns. Peak fractions containing the expressed proteins were further purified on an anion-exchange Mono Q or Mono S columns.

Determination of Physical Properties of Recombinant Polypeptides

Sedimentation coefficients (S$_{20,w}$) of each bacterially expressed polypeptide were determined by rate-zonal sedimentation at 40,000 rpm for 14 h at 4°C in a SW 50.1 rotor on 5–20% linear sucrose gradients (Martin and Ames, 1961) in a buffer containing 10 mM sodium phosphate, 100 mM NaCl, 1 mM NaEDTA, 1 mM NaN$_3$, and 0.5 mM DTT. Standards included bovine liver catalase (11.3 S$_{20,w}$), rabbit muscle aldolase (7.3 S$_{20,w}$), bovine serum albumin (4.6 S$_{20,w}$), and horse heart cytochrome C (1.75 S$_{20,w}$). Stokes radii (Rs) were estimated by gel filtration on a Superose 12 column equilibrated with a buffer containing 1 M NaBr, 10 mM sodium phosphate, 1 mM NaEDTA, 1 mM NaN$_3$, 0.5 mM DTT, and 0.05% Tween-20 and calibrated with standard proteins: bovine serum albumin (3.5 nm), ovalbumin (2.8 nm), and horse heart cytochrome C (0.2 nm).

Circular dichroism was measured with a Jobin-Yvon Dichrograph Mark V instrument which was interfaced with an Apple IIC computer. Data was taken at 0.5-nm intervals with one second response time. Spectra were taken at 4°C with protein concentration at 50 μg/ml in 1 mM Tris and 0.4 M NaF, pH 7.4. This buffer was selected based on solubility requirements of the control protein, a 43-kD polypeptide derived from the membrane-binding domain of erythrocyte ankyrin (Michaely and Bennett, 1993).

Antibody Preparation

Polyclonal antiserum was raised using one of the expressed polypeptides (λ606) as an immunogen in rabbit. Procedures used for affinity purification of antibody were as described (Davis and Bennett, 1990). Antibody specific for the 440-kD ankyrin_B was eluted from the affinity column with 4 M MgCl$_2$ and dialyzed against 20% (wt/vol) sucrose, 150 mM NaCl, 10 mM sodium phosphate, 1 mM NaEDTA, and 1 mM NaN$_3$ and stored at −70°C in aliquots. The quality of antibody was tested by immunoblotting using total bovine brain membrane polypeptides. Previously described 440-kD ankyrin_B antibody was also used in some experiments (Kunimoto et al., 1991).

Immunoblotting and Immunofluorescence

Optic nerves of neonatal and adult Sprague-Dawley rats were dissected and homogenized in 0.32 M sucrose, 2 mM NaEGTA and 1 mM NaN$_3$ buffer with 10 μg/ml pepstatin, leupeptin, 0.01% diisopropyl fluorophosphate, and 100 μg/ml phenylmethylsulphonyl phosphate. An equal volume of 5×

PAGE buffer was added to the homogenate and samples electrophoresed on a 3.5–17% exponential gradient SDS-PAGE gel (Davis and Bennett, 1983). Polypeptides were electrophoretically transferred to nitrocellulose paper and immunoblotted with either a 440-kD ankyrin$_B$-specific antibody, or anti-myelin basic protein monoclonal antibody using ^{125}I-labeled protein A to detect bound Ig (Davis and Bennett, 1983). The amounts of protein loaded on gel were compared in different samples by elution of dye from Coomassie blue-stained gels with 25% pyridine followed by measurement of absorbance at 550 nm.

For immunofluorescence studies, postnatal day 2 and adult Sprague-Dawley rats of *Shiverer* mice were perfused first with heparin (30 U/ml) in phosphate-buffered saline, followed by 2% paraformaldehyde in 0.1 M sodium phosphate, pH 7.5. Optic nerves from rats and the forebrain, the cerebellum and the brain stem of the *Shiverer* mice were removed and placed in the same fixative for 2 h. Tissues were cryoprotected in 5% sucrose for 2 h, 10% sucrose for 2 h, and 25% sucrose overnight, and were frozen in liquid nitrogen-cooled isopentane. For 1-μm rat optic nerve sections, the tissues were prepared as previously described (Kordeli et al., 1990) and cut by an ultracryomicrotome at − 80°C and mounted on polylysine-coated glass slides. For samples of the *Shiverer* mouse brain, 4–10 μm sections were cut in a microtome at − 20°C. Sections were incubated with 5 μg/ml 440-kD ankyrin$_B$ antibody with 0.05% Tween-20 overnight at 4°C and washed with PBS several times as described (Kordeli et al., 1990). Ig molecules were visualized with affinity-purified rhodamine-conjugated goat anti-rabbit antibody.

Electron Microscopy

The rat optic nerve was dissected from brain and placed in 4% paraformaldehyde and 2.5% glutaraldehyde in 0.1 M Na phosphate buffer, pH 7.5 overnight. The fixed tissue was washed several times with PBS, postfixed for 2 h with 1% osmium tetroxide reduced with potassium ferrocyanide immediately prior use, dehydrated with a graded ethanol and embedded in Spurr resin, cut with a diamond knife at 70–90 nm, post stained with uranyl acetate and lead citrate, and viewed in a Philips EM 300 electron microscope.

Results

Analysis of cDNA Clones Encoding the Inserted Sequence of 440-kD Ankyrin$_B$

cDNA clones located at the 5′ and 3′ ends of the inserted sequence of 440-kD ankyrin$_B$ (Otto et al., 1991) were used as probes to obtain cDNA clones for the remainder of this region by screening a human fetal brain stem cDNA library. Two overlapping cDNA clones were isolated (Fig. 2 *A*), which, together with clones obtained by Otto et al. (1991), completed the inserted sequence. The inserted sequence of 2,085 amino acids is encoded by 6,255 base pairs of cDNA (Fig. 2 *B*). The calculated molecular mass based on the amino acid sequence of this inserted region is 228.6 kD, a value which agrees well with the predicted molecular mass of 220 kD based on the M_r of 440-kD ankyrin$_B$ on SDS-gels (Kunimoto et al., 1991). The calculated molecular weight of the full length 440 ankyrin$_B$ based on cDNA sequence is 431 kD. An important caveat is that the polypeptides may contain additional insertions/deletions. Until this uncertainty is resolved by analysis of a full length cDNA, we will continue to refer to the polypeptide as 440-kD ankyrin$_B$.

The inserted sequence is acidic (pI of 4.5) and highly enriched in hydrophilic residues. The inserted sequence is also enriched in proline residues (8%). A hydrophilicity profile of this sequence exhibits few stretches of hydrophobic sequence (Fig. 3 *A*). The hydrophilicity profile of the globular spectrin and membrane binding domains, in contrast (Fig. 3 *B*), exhibits alternating hydrophobic and hydrophilic stretches, as is typical of globular proteins. The COOH-

A

B
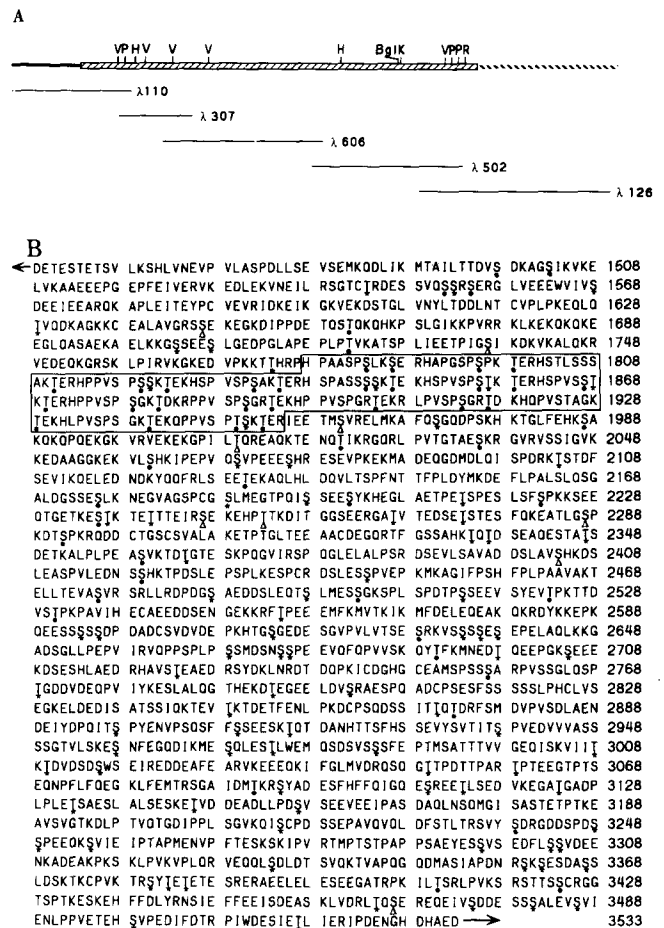
Figure 2. Overlapping cDNA clones and the amino acid sequence coding for the 440-kD ankyrin$_B$ inserted sequence. (*A*) Alignment of the overlapping cDNA clones for 440-kD ankyrin$_B$ inserted sequence. The insert region is cross-hatched and boxed. Restriction sites are shown as: *Bgl*, Bgl II; *R*, EcoRI; *H*, HindIII; *K*, KpnI; *P*, PstI; *V*, PvuII. Individual clones are numbered on the right. (*B*) Derived amino acid sequence of the 440-kD ankyrin$_B$ insert region. 2,085 amino acids were deduced from the cDNA sequence. The first and last amino acid represent the start and end of the insert region. Potential protein phosphorylation sites for protein kinase C, casein kinase 2, and for both kinases are indicated by dot, star, and triangle, respectively. The 15 12-amino acids unique repeats (r1-r15) are boxed. The number on the right represents the amino acid number corresponding to the entire 440-kD ankyrin$_B$. These sequence data are available from EMBL/Genbank/DDBJ under accession number Z26634.

terminal domain shared by 440- and 220-kD ankyrin$_B$ isoforms (the last 330 amino acids) also exhibits a hydrophilic profile similar to that of the inserted sequence. Secondary structure analysis by the Chou-Fasman algorithm predicts little β sheet or α helix and mainly turns (not shown). These properties suggest that a major portion of the inserted amino acid sequence lacks globular structure.

The inserted amino acid sequence contains many potential phosphorylation sites for protein kinases (Fig. 2 *B*). This region contains 97 potential sites for phosphorylation by casein kinase 2, 69 sites for protein kinase C, 54 sites for proline-directed protein kinase, and 5 sites for cAMP-
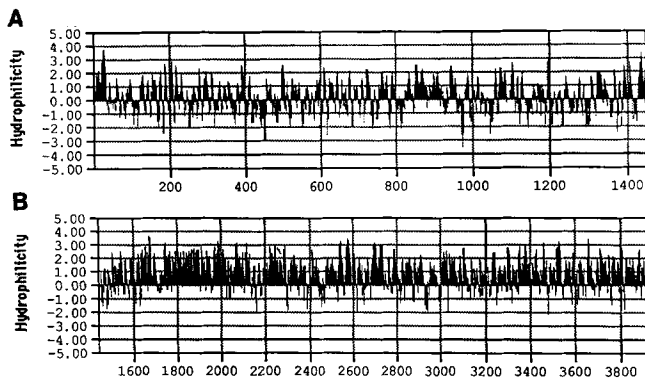
Figure 3. The hydrophilicity profile of (*A*) the spectrin and membrane binding domains and (*B*) the inserted sequence (amino acid 1448–3533) of the 440-kD ankyrin$_B$ and the common COOH-terminal domain (amino acid 3534–3925) of ankyrin$_B$. Number at the bottom indicates the amino acid.

dependent protein kinase. Potential sites for phosphorylation by protein kinase C and proline-directed protein kinase are concentrated at the amino terminus of the inserted sequence. The NH₂-terminal region contains 15 copies of a 12–amino acid repeat with the consensus of his-pro-pro-val-ser-pro-ser-X-lys-thr-glu-lys (Fig. 2 *B*) (Otto et al., 1991). Each repeat has two potential phosphorylation sites for protein kinase C as well as proline-directed protein kinase (Vulliet et al., 1989). Potential casein kinase 2 phosphorylation sites are distributed throughout the inserted sequence.

A search for related amino acid sequences did not reveal an exact match between the inserted sequence and any reported protein. However, similarities were noted between the inserted sequence and those of microtubule-associated protein 1B, and neurofilament H. MAP 1B contains a stretch of sequence (from residue 322 to 2464) with 39% similarity by BestFit analysis. MAP 1B is a major component of the neuronal cytoskeleton (Bloom et al., 1985), and has a filamentous tail (average 186 nm in length) in addition to a globular head 10 nm in diameter (Sato-Yoshitake et al., 1989). Mouse neurofilament H subunit has 42% similarity (from residues 9 to 831) to the inserted sequence of 440-kD ankyrin$_B$ (from residues 1448–2228) by BestFit analysis. Neurofilament H subunit also has a thin, filamentous configuration (Hisanaga and Hirokawa, 1988).

Physical Properties of Inserted Sequence of 440 Ankyrin$_B$

The lack of hydrophobic stretches in the inserted sequence, abundance of proline residues, and similarity to sequences of filamentous proteins MAP 1B and neurofilament H suggest that the inserted sequence may have a nonglobular and possibly extended structure. To directly examine properties of 440-kD ankyrin$_B$, we attempted to purify the native protein from bovine brain. Unfortunately, isolation of 440-kD ankyrin$_B$ has not yet been achieved due to technical problems that include low yields and incomplete dissociation of 440-kD ankyrin$_B$ from other proteins. An alternative strategy was to express this sequence in bacteria and determine physical properties of recombinant polypeptides. More than 75% of the inserted sequence was expressed in *E. coli*, and
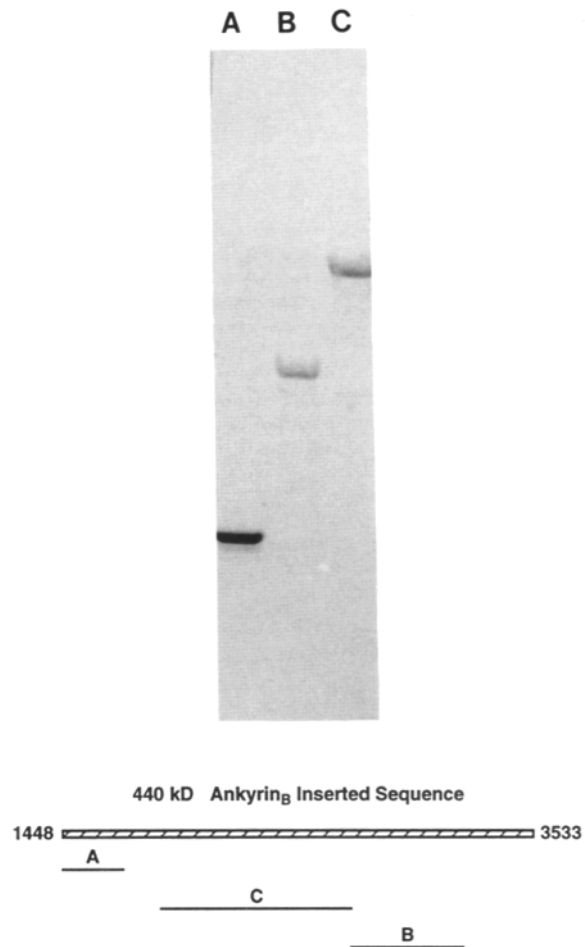
Figure 4. Coomassie blue staining of the bacterially expressed polypeptides comprising 175 kD of the inserted sequence of 440-kD ankyrin$_B$. Expressed proteins were run on 3–17% exponential gradient polyacrylamide SDS gel. (Lane *A*) Amino acids 1455–1711; (lane *B*) amino acids 2875–3370; (lane *C*) amino acids 2054–2876. Schematic map at the bottom indicates the corresponding expressed polypeptides.

individual expressed proteins were purified to homogeneity (Fig. 4). Identity of recombinant proteins was verified by NH₂ terminal sequence analysis (data not shown).

Sedimentation coefficients and Stoke's radii of recombinant polypeptides were experimentally determined, and these values were used to calculate frictional coefficients. The two largest polypeptides, encompassing 70% of the inserted sequence, have frictional coefficients of 2.4 and 1.9, respectively, indicating that both polypeptides have a highly asymmetrical shape. Values for molecular weight for the two expressed polypeptides calculated from hydrodynamic values (λ606 = 101 kD and λ502 = 42 kD) are close to the actual molecular weights based on amino acid sequence (λ606 = 90 kD and λ502 = 55 kD, indicating that the expressed polypeptides are monomers. The apparent molecular weights estimated by mobility on SDS-PAGE for expressed λ606 and λ502 were 125,000 and 77,900, respectively. Anomalous migration on SDS-PAGE gels may be due to reduced binding to SDS to these hydrophilic and highly charged polypeptides. One polypeptide of 220 residues en-

Table I. Physical Properties of Bacterially Expressed Polypeptides Derived from the Inserted Sequence of 440-kD Ankyrin$_B$

Properties	Constructs		
	λ606	λ502	λ110
Stokes Radius, R$_s$* (nm)	7.8	5.2	2.7
Sedimentation coefficient,‡ $s_{20,w}$	3.1	1.9	2.1
Partial specific volume,§ $\bar{v}$	0.73	0.73	0.73
MW, calculated‖	101K	42K	24K
MW based on amino acid sequence	90K	55K	21K
M$_r$, by SDS-PAGE	125K	78K	20K
Frictional ratio, f/f_0‖	2.4	1.9	1.3

* Determined from gel filtration on superose 12 column (see Materials and Methods).
‡ Determined from 5–20% linear sucrose gradient (see Materials and Methods).
§ Estimated from amino acid composition (Cohn and Edsall, 1943).
‖ Calculated according to equations (Tanford, 1961).

$$M_r = \frac{6\pi N R_s s_{20,w}}{1 - v\rho_{20,w}}$$

and

$$f/f_0 = R_s \left(\frac{4\pi N}{3M_r (v + \delta\rho)} \right)^{1/3}$$

where δ was assumed to be 0.2 g of solvent/g of protein.

Figure 5. Circular dichroism spectra of bacterially expressed polypeptides derived from the inserted sequence of 440-kD ankyrin$_B$. *A, B,* and *C* represent the same polypeptides shown in Fig. 4. The control protein (*D*) is the 43-kD fragment of erythrocyte ankyrin which are prepared in a similar procedure. Typical CD spectra for a random coiled protein is represented by a negative peak at 200 nm. Typical CD spectrum for an α-helix protein is represented by two negative peaks at 222 nm and 208 nm. All samples were prepared as described in the Materials and Methods. The spectra of 43-kD fragment of erythrocyte ankyrin was kindly provided by Peter Michealy.
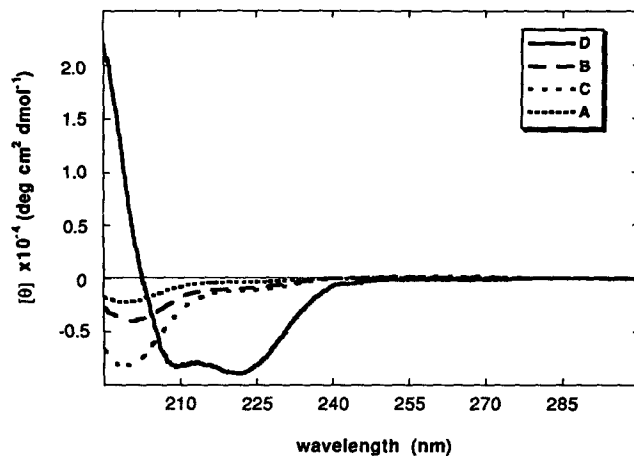
coded by sequence adjacent to the spectrin-binding domain exhibited a frictional ratio of 1.3 (Table I), and therefore is approximately spherical.

Circular dichroism spectra of recombinant polypeptides were determined in order to evaluate secondary structure (Fig. 5). The two largest polypeptides exhibit spectra consistent with a random-coiled configuration with an intense negative peak at 200 nm, and little signal at higher wavelengths. A negligible (<1%) fraction of α-helix for all three expressed polypeptides was estimated using the equation provided by Chen et al. (Chen and Yang, 1971). In contrast, the spectrum of a 43-kD polypeptide derived from the membrane-binding domain of ankyrin$_R$, also expressed in bacteria, exhibits a signal corresponding to 26% α-helix (Fig. 5). 43-kD ankyrin$_R$ is a portion of ankyrin$_R$ in the globular membrane binding domain which gives nearly identical CD spectra as the native 89-kD membrane binding domain (Michaely and Bennett, 1993).

Heat stability of the expressed polypeptides provides additional evidence for nonglobular folding. These proteins still remained soluble after incubation at 100°C for 10 min (Fig. 6). Other cytoskeletal proteins that are heat-stable and have an elongated structure include microtubule-associated protein 2 (MAP2) (Voter and Erickson, 1982) and tau protein (Fellous et al., 1977).

Expression of 440-kD Ankyrin$_B$ in Developing Rat Optic Nerve

Unresolved questions from previous work include whether 440-kD ankyrin$_B$ is localized in axons, and if the down-regulation of expression of 440-kD ankyrin$_B$ after postnatal day 10 is related to myelination of axons. Rat optic nerve pro-

vides a system well suited to approach these issues. The neonatal optic nerve is comprised almost entirely of unmyelinated axons with few glial cells and no dendrites (Black et al., 1982; Skoff et al., 1976*a,b*). In addition, the optic nerve represents axons from a single layer of neurons (ganglion cells) in the retina which are completely myelinated in a well defined time period (see Fig. 9 *F*). The ganglion cell dendrites also makes synapses with axons (bipolar cell axons)
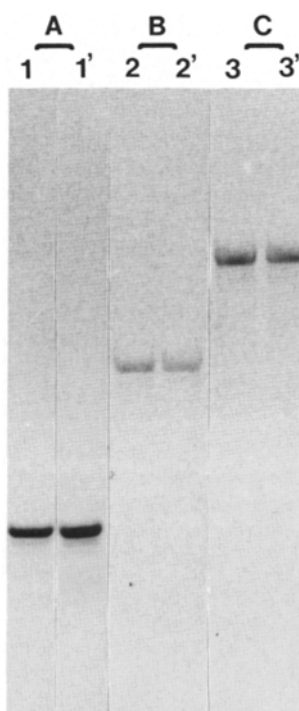
Figure 6. The inserted sequence of the 440-kD brain ankyrin$_B$ is heat stable. Expressed polypeptides (same *A, B,* and *C* as in Fig. 4) were boiled in a water bath for 10 min and centrifuged for 10 min in a microfuge. Starting polypeptides (lanes *A1, B2,* and *C3*) and supernatants after heating and centrifugation (lanes *A1', B2',* and *C3'*) were analyzed on a SDS-PAGE gel.
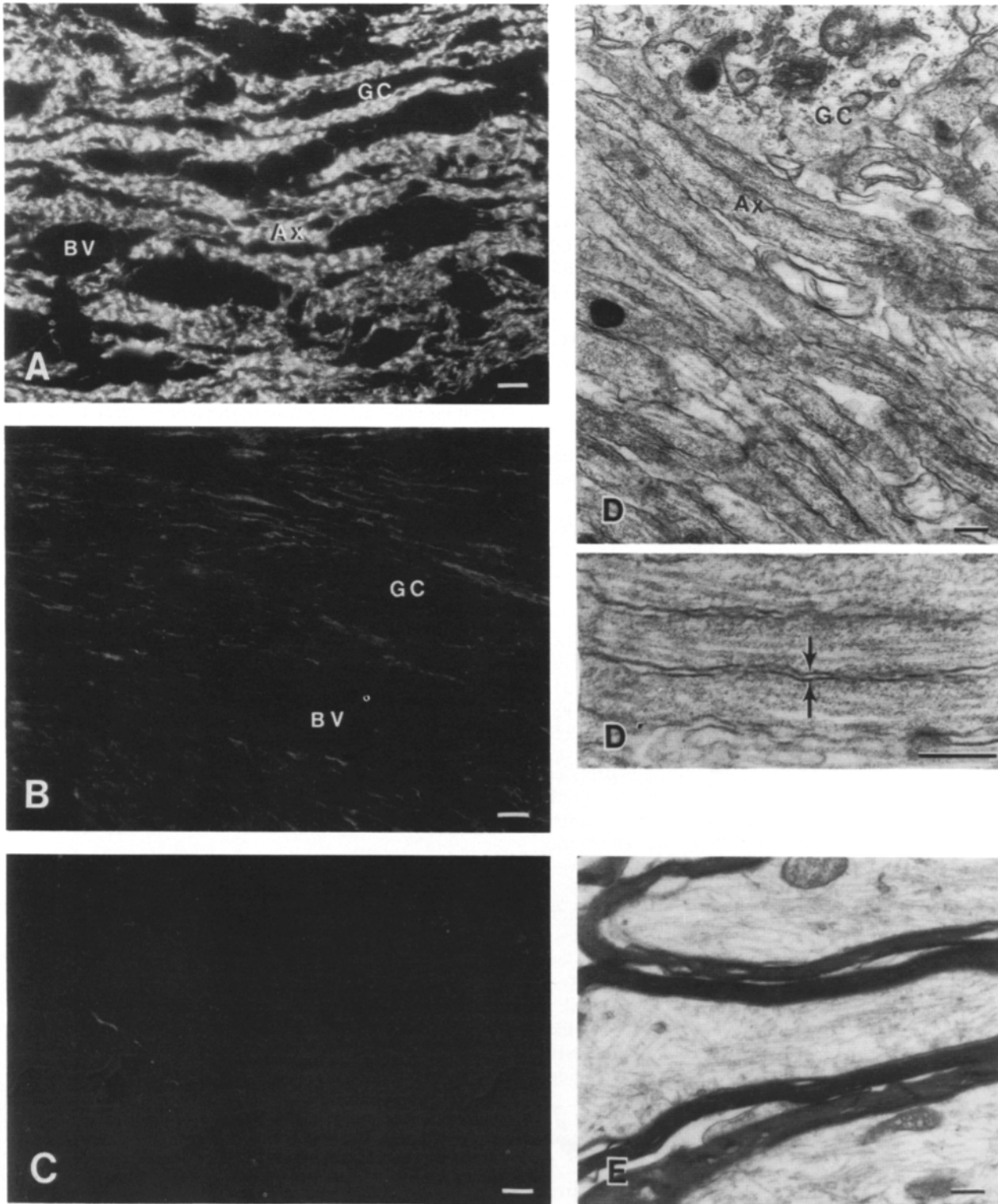
Figure 7. 440-kD ankyrin$_B$ is highly expressed in unmyelinated axons in rat optic nerve. 1-μm cryosections of rat optic nerve were stained with the 440-kD ankyrin$_B$-specific antibody. (*A*) Postnatal day 2; (*B*) postnatal day 14; (*C*) adult. (*D*) Electron micrograph of the pre-myelinated axons in the postnatal day 2 optic nerve is shown in low magnification (*D*) and high magnification (*D'*). Arrows in *D'* indicate the axonal membrane and the absence of myelin. (*E*) Electron micrograph of myelinated axons in adult rat optic nerve. *GC* glial cells; *Ax*, axons; *BV*, blood vessels. Bars: (*A, B,* and *C*) 10 μm; (*D* and *D'* and *E*) 0.2 μm.

from another layer of neurons called interneurons (see Fig. 9 E). At postnatal day 2, the optic nerve is mainly composed of bundles of unmyelinated axons (Fig. 7, D and D'). At postnatal day 14, myelination has proceeded to an advanced stage and is completed in adults, (Fig. 7 E) (Black et al., 1982). Therefore, immunostaining of sections from different developmental stages of optic nerve and retina provides information regarding localization of 440-kD ankyrin$_B$ and correlation of myelination with expression of this protein.

Antibody against the 440-kD ankyrin$_B$ exhibited intense immunofluorescent staining of the optic nerve in postnatal day 2 rat optic nerve (Fig. 7 A). Immunofluorescence staining of optic nerve decreased dramatically at postnatal day 14 (Fig. 7 B), and almost disappeared in adult (more than 6 wk) nerve (Fig. 7 C). Quantitative immunoblots of optic nerves demonstrate that the amount of 440-kD ankyrin$_B$ decreases between day 13 and 16, with only around 7% remaining in adult optic nerve (Fig. 8). Myelination during these developmental stages was followed by immunoblot analysis with antibody against myelin basic protein. Expression of myelin basic protein in rat optic nerve occurred in parallel with loss of 440-kD ankyrin$_B$ (Fig. 8). These results suggest two conclusions: first, that 440-kD ankyrin$_B$ definitely is localized in unmyelinated axons, and second, disappearance of 440-kD ankyrin$_B$ from axons is closely coordinated with the process of myelination.

Neurons that contribute the axons of the optic nerve are concentrated in a single layer of the retina (Fig. 9 E). The cell bodies of these neurons as well as their dendrites do not exhibit detectable staining with antibody against 440-kD ankyrin$_B$ at day 2 (Fig. 9 A), a time when the optic nerve exhibits intense staining (Fig. 7 A). Moreover, immunoblot analysis of retina also reveals undetectable expression of 440-kD ankyrin$_B$ at day 2 (Fig. 9 D). Control experiments using an antibody against a spliced variant of ankyrin$_R$ clearly shows staining in the cell bodies and dendrites (Fig. 9 C) (Kordeli and Bennett, 1991). These observations suggest that 440-kD ankyrin$_B$ is highly concentrated in axons and is absent from cell bodies and dendrites of neurons that form the optic nerve.

440-kD Ankyrin$_B$ Elevated in Nerve Tracts of Myelin-deficient Shiverer Mice

The finding that disappearance of 440-kD ankyrin$_B$ from axons occurs at the same time as myelination suggests the possibility that myelination could actually cause the loss of 440-kD ankyrin$_B$. Myelin-deficient mutant mice *Shiverer* provide an excellent model to test this idea. *Shiverer* is an autosomal recessive mutant with a myelin deficiency of the central nervous system due to deletion of the gene encoding myelin basic protein (Chernoff, 1981; Kimura et al., 1985). In the *Shiverer* mutant, the major dense line of myelin does not form (Inoue et al., 1981), although the peripheral nervous system of *Shiverer* mice appears almost normal (Mikoshiba et al., 1981). The central nerve tracts are mostly unmyelinated in the *Shiverer* mice (Bird et al., 1978; Rosenbluth, 1980). Levels of 440-kD ankyrin$_B$ are elevated in the central nerve tracts of *Shiverer* in both the forebrain and cerebellum (Fig 10, B and D) as compared with those of control mice based on immunofluorescence staining (Fig. 10, A and C). These results support the hypothesis that myelination actually causes loss of 440-kD ankyrin$_B$ from axons. Mossy fibers of the hippocampus also contain unmyelinated axons in normal mice and these areas exhibit strong staining with 440-kD ankyrin$_B$ antibody (Fig. 10, A and B).
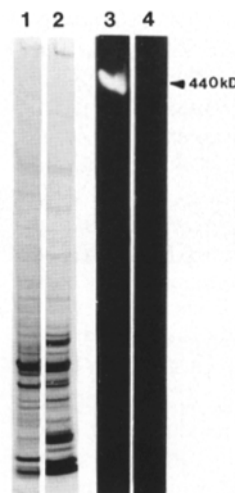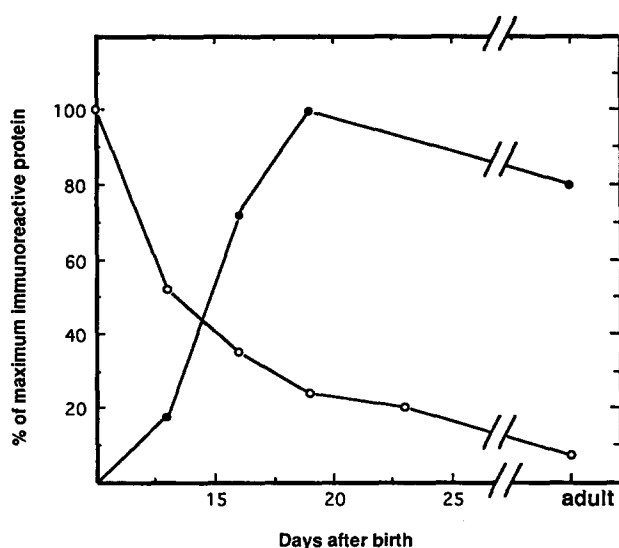
Figure 8. Quantitative determination of the expression 440-kD ankyrin$_B$ in developing rat optic nerve. Total homogenates of rat optic nerve from postnatal days 10, 13, 16, 19, and 23 were separated on SDS-PAGE gel, transferred to nitrocellulose membrane and immunoblotted using ^{125}I-labeled protein A and 440-kD ankyrin$_B$-specific antibody and monoclonal antibody against myelin basic protein (MBP). Amounts of immunoreactivity were compared by densitometry of autoradiograms, and these values were normalized with respect to protein, which was estimated by elution of dye from Coomassie blue–stained gels with 25% pyridine followed by measurement of absorbance at 550 nm. The ratio of immunoreactivity/protein is expressed as percent of maximum value. (Lanes *1-2*) Coomassie blue–stained gel sample of 2-d-old (lane *1*) and adult (lane *2*) rat optic nerve. (Lane *3-4*) Same samples in lanes *1* and *2* were transferred to nitrocellulose membrane and blotted with 440 ankyrin$_B$-specific antibody.
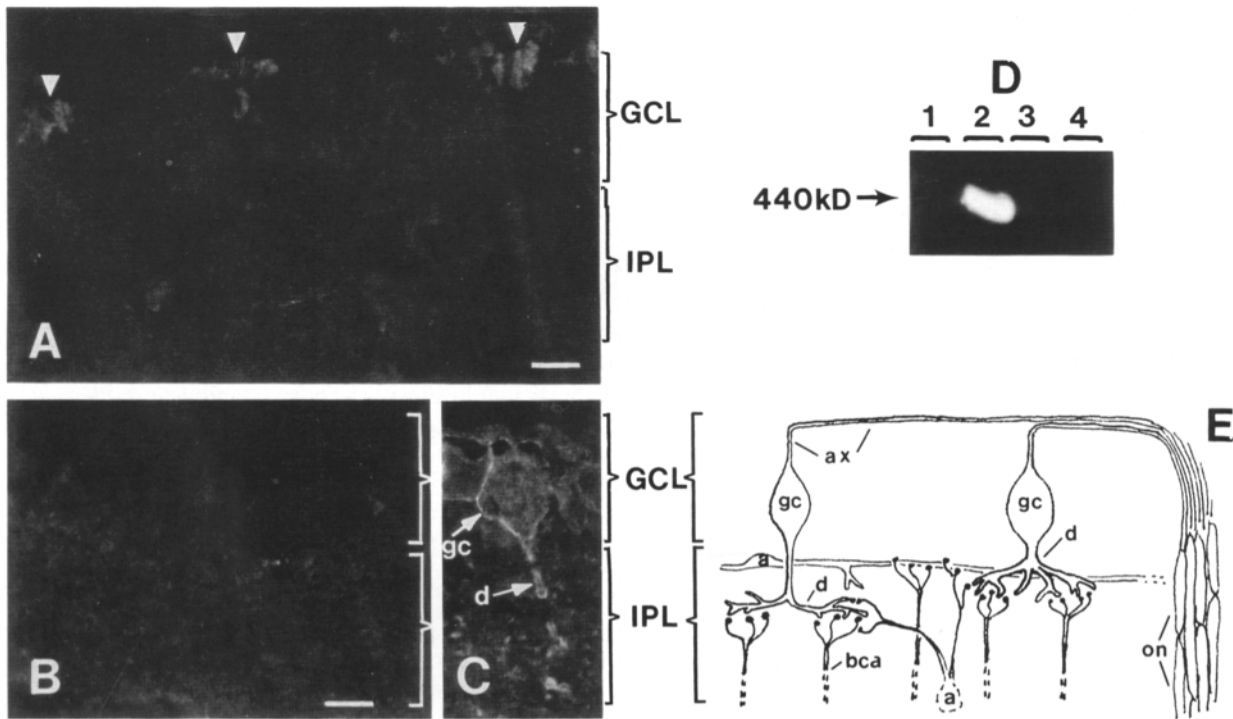
Figure 9. 440-kD ankyrin_B is highly concentrated in axons and is absent from cell bodies and dendrites of ganglion neurons in the rat retina. 1-μm thin sections of 2-d-old (*A* and *C*) and adult (*B*) rat retina layer were immunostained with 440-kD a ankyrin_B-specific antibody (*A* and *B*) and ankyrin_{Ro} (*C*) which is immunologically related to ankyrin_R (Kordeli and Bennett, 1991). 440-kD ankyrin_B antibody does not stain cell bodies and dendrites either in 2-d-old or adult retina (*A* and *B*) whereas ankyrin_{Ro} antibody brightly stain the cell bodies and dendrites (*gc* and *d* in *C*). The arrowheads in *A* indicate the bundles of ganglion cell axons. (*D*) Lane *1*, adult optic nerve. Lane *2*, 2-d-old optic nerve. Lane *3*, adult retina. Lane *4*, 2-d-old retina. Samples were immunoblotted with 440 ankyrin_B-specific antibody. (*E*) A simplified schematic drawing of the retina and optic nerve. *gc*, ganglion cell; *a*, amacrine cell; *ax*; ganglion cell axons; *d*, ganglion cell dendrites; *bca*, bipolar cell axons; *on*, optic nerve; *GCL*, ganglion cell layer; *IPL*, inner plexiform layer. Bars, 10 μm.

Discussion

This paper reports the sequence of 2,085 amino acids inserted between the membrane/spectrin binding and COOH-terminal domains of 440-kD ankyrin_B as the result of developmentally regulated splicing of pre-mRNA. Notable features of the inserted sequence, in addition to its length, include a hydrophilicity profile that contains few hydrophobic regions, and 220 predicted sites for phosphorylation by protein kinases (casein kinase 2, protein kinase C, and proline-directed protein kinase). Polypeptides corresponding to 70% of the inserted residues were expressed in bacteria and determined to have properties of an extended, random coil. Frictional coefficients were 1.9–2.4, indicating a highly asymmetric shape. Circular dichroism spectra indicate that the inserted sequence is nonglobular with negligible alpha helix or beta sheet structure. Moreover, the expressed polypeptides were resistant to boiling, another property consistent with a nonglobular structure.

Properties of the inserted sequence suggest a ball and chain physical model for both 220- and 440-kD ankyrin_B with globular head domains, and extended filamentous tail domains comprised of COOH-terminal residues (Fig. 11). The tail domain of 220-kD ankyrin_B in this model is comprised of the COOH-terminal 330 residues, while the tail domain of 440-kD ankyrin_B includes 2,085 residues in the inserted sequence as well as the 330 COOH-terminal residues

also present in 220-kD ankyrin_B. Experimental evidence for an extended conformation for the shared COOH-terminal domain is that 220-kD ankyrin_B has a frictional ratio of 1.6 (Davis and Bennett, 1984a), reflecting asymmetry in the molecule that is not due to the spectrin/membrane binding domains (Hall and Bennett, 1987). Additional features consistent with an extended conformation of the common COOH-terminal domain is that hydrophilicity plots of this sequence are similar to the inserted sequence in the lack of hydrophobic stretches. The globular membrane/spectrin binding domain has a diameter of 11–12 nm based on the Stokes radius of the spectrin/membrane-binding domain of ankyrin_R (Hall and Bennett, 1987). The tail domain of 440-kD ankyrin_B contains 2,415 residues and is predicted to be ∼217 nm in length based on experimentally observed lengths of random coil polypeptides of comparable size. MAP2, for example contains 2,000 amino acids (Wang et al., 1988) and is 180 nm in length (Voter and Erickson, 1982) while MAP1B contains 2,464 amino acids (Noble et al., 1989) and has a 10-nm head domain and a tail 186 nm in length (Sato-Yoshitake et al., 1989).

The ball and chain model for 440- and 220-kD ankyrin_B (Fig. 11) suggests the hypothesis that the predicted tail domains have structural roles involving interaction with cytoskeletal and/or peripheral membrane components. The predicted length of 217 nm for the tail of 440-kD ankyrin_B
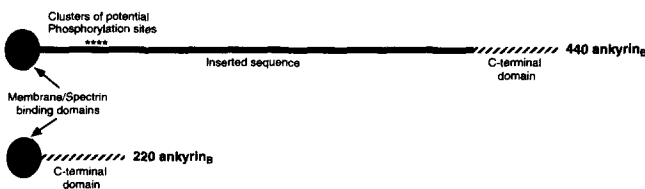
1470
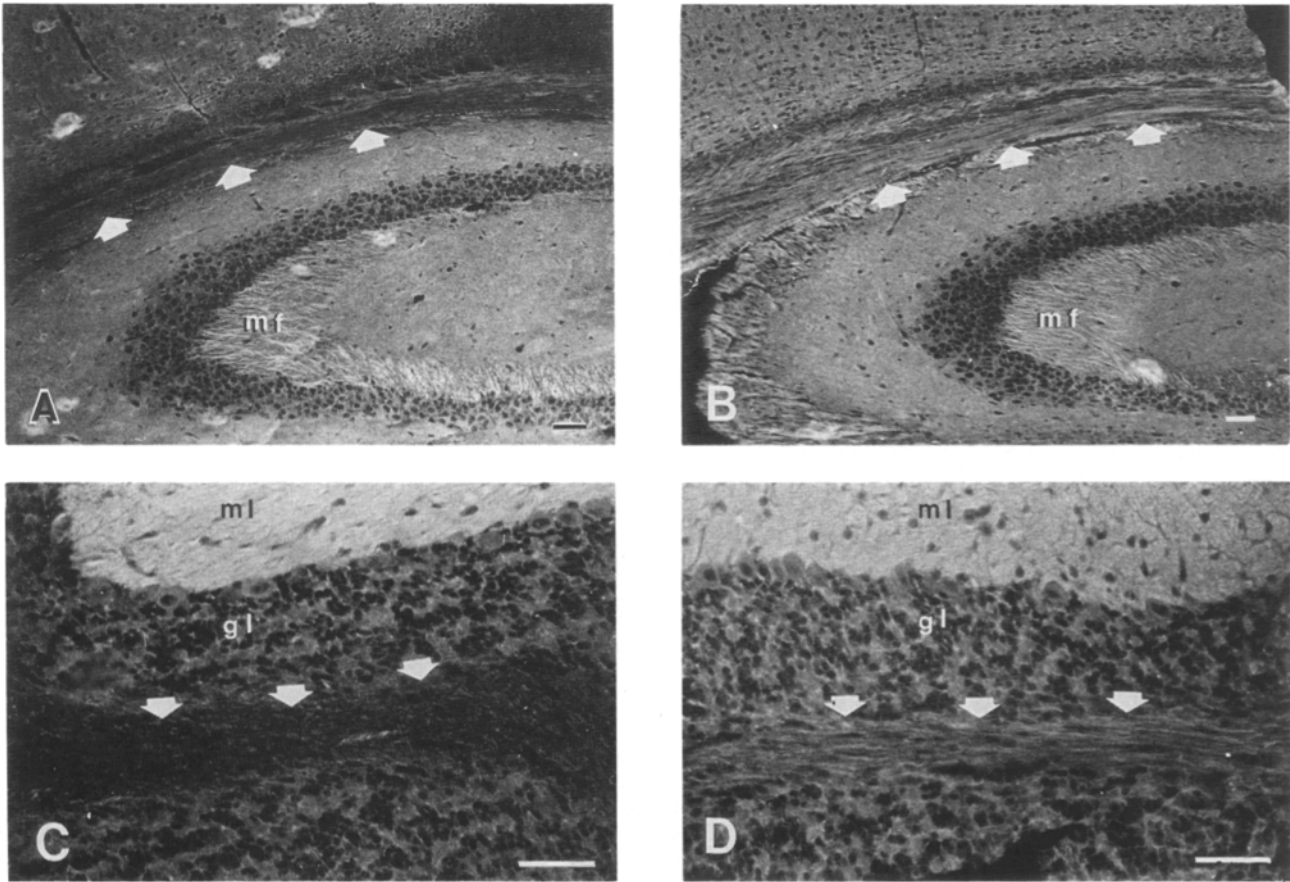
Figure 10. Expression of 440-kD ankyrin_B is elevated in the central nerve tracts of myelinate-deficient mouse *Shiverer.* 10-μm cryosections of forebrain (*A* and *B*) and cerebellum (*C* and *D*) from Shiverer (*B* and *D*) and control mice (*A* and *C*) were stained with 440-kD ankyrin_B-specific antibody (see Materials and Methods). Large arrows indicate the white matter nerve tracts in the forebrain and cerebellum. *mf*, mossy fibers of hippocampus are intensely stained. *ml*, molecular layer of the cerebellum. *gal*, granular layer of the cerebellum. Bars, 50 μm.

is sufficient to extend a significant fraction of the diameter of an unmyelinated axon (200–300 nm in the case of optic nerve (Pachter and Liem, 1984), and would be available for interactions with microtubule or intermediate filament-based structures. The extended tail could also lie parallel to the plasma membrane and associate with peripheral membrane proteins. It will be important in future experiments to determine if the inserted sequence or the COOH-terminal residues shared by 440- and 220-kD ankyrins interact with cytoplasmic proteins and/or peripheral membrane proteins.

The large number of potential phosphorylation sites in the inserted sequence suggests the possibility that phosphorylation may play a role in regulating the structure and function of 440-kD ankyrin_B. Other structural proteins localized in

Figure 11. A schematic model for 440- and 220-kD brain ankyrin.

axons that are targets for various protein kinases at multiple sites include tau protein (Correas et al., 1992), neurofilament subunits (Julien and Mushynki, 1982; 1983; Sterberger and Sternberger, 1983), and MAP1B (Diaz-Nido et al., 1988; Hoshi et al., 1990). It will be of interest to determine if 440-kD ankyrin_B actually is phosphorylated in vivo, and to elucidate consequences of phosphorylation.

440-kD ankyrin_B is selectively targeted to unmyelinated axons, based on the observations that this protein is present in premyelinated axons of neonatal rat optic nerve, and is absent from the cell bodies and dendrites of neurons that form optic nerve axons (Figs. 8–10). Other proteins known to be selectively targeted to axons include GAP-43 (Goslin et al., 1988, 1990; Meiri et al., 1986), and certain isoforms of tau (Binder et al., 1985). 440-kD ankyrin_B is lost in parallel with myelination of the optic nerve, and is retained in nerve tracts of *Shiverer* mice, which do not form compact myelin. These observations suggest the hypothesis that myelination somehow causes loss of expression of 440-kD ankyrin_B. It will be of interest to determine the nature of intercellular signaling between neurons and oligodendrocytes leading to downregulation of expression of 440-kD ankyrin_B. Additional issues raised by these findings include the mechanism of targeting and function of 440-kD ankyrin_B in axons.

Disappearance of 440-kD ankyrin$_B$ from axons after myelination of the optic nerve closely parallels behavior of the nervous cell adhesion molecule L1, which also is lost from optic nerve during myelination in mouse (Bartsch et al., 1989) and fish (Blaugrund et al., 1992). L1 may also have ankyrin-binding activity, since the cytoplasmic domain of L1 exhibits 50% sequence identity with the cytoplasmic domains of a recently described family of ankyrin-binding glycoproteins expressed in adult brain (Davis et al., 1993). These considerations suggest the possibility that L1 and 440-kD ankyrin$_B$ may associate in unmyelinated axons. L1 is believed to participate in associations between unmyelinated axons resulting in bundles or fascicles of axons (Fischer et al., 1986). A linkage between L1 and 440-kD ankyrin$_B$ with its extended tail domain could potentially provide a transcellular connection between cytoskeletal structures and extracellular domains of L1 on adjacent axons. Such a series of linkages involving L1 and 440-kD ankyrin$_B$ would mechanically stabilize unmyelinated axons, and would need to be removed in order for axons to be enveloped by myelin. To evaluate these ideas, it will be necessary to determine if L1 actually has ankyrin-binding activity, and if retention of 440-kD ankyrin$_B$ and L1 in axons prevents myelination.

GAP-43 exhibits several similarities to 440-kD ankyrin$_B$. GAP-43 is much more concentrated in developing nerve tissue than adult nervous tissue (Meiri et al., 1986) and is specifically targeted to axons (Goslin et al., 1988, 1990). The fact that GAP-43 and 440-kD ankyrin$_B$ are localized in axons suggests that both proteins may contain common epitope(s) for such a targeting event. Comparison of GAP-43 sequence and 440 ankyrin$_B$ sequence shows several short stretches of sequence similarity in residues 1748-2048 in 440-kD ankyrin$_B$ (data not shown). It will be of interest to determine if the sequence similarities between GAP-43 and 440-kD ankyrin$_B$ reflect a common mechanism for targeting of these proteins to axons, or possibly interaction with a common class of axonal proteins present in premyelinated axons.

Different members of the ankyrin gene family presumably evolved by gene duplication events, beginning with a primordial ankyrin. The inserted sequence of 440-kD ankyrin$_B$, which is missing in ankyrin$_R$, was therefore either added through gene fusion or deleted by unequal recombination events during evolution. If the initial ankyrin gene contained an extended tail domain, it would be predicted that newly discovered ankyrin genes may also include tail domains as well. In this case, the current view of ankyrin function may be incomplete and biased due to the reliance on studies of ankyrin$_R$ and 220-kD ankyrin$_B$ which lack extended tail domains.

References

Bartsch, U., F. Kerchief, and M. Stationer. 1989. Immunohistological localization of the adhesion molecules L1, N-CAM, and MAG in the developing and adult optic nerve of mice. *J. Comp. Neurol.* 284:451–462.

Baskins, G. S., and R. G. Langdon. 1981. A spectrin-dependent ATPase of the human erythrocyte membrane. *J. Biol. Chem.* 256:5426–5435.

Bennett, V. 1978. Purification of an active proteolytic fragment of the membrane attachment site for human erythrocyte spectrin. *J. Biol. Chem.* 253:2292–2299.

Bennett, V. 1992. Ankyrins: adaptors between diverse plasma membrane proteins and the cytoplasm. *J. Biol. Chem.* 267:8703–8706.

Binder, L. I., A. Frankfurter, and L. I. Rebhun. 1985. The distribution of tau in the mammalian central nervous system. *J. Cell Biol.* 101:1371–1378.

Bird, T. D., F. D. F., and S. M. Sumi. 1978. Brain lipid composition of the Shiverer mouse: genetic defect in myelin development. *J. Neurochem.* 31:387–391.

Black, J. A., R. E. Foster, and S. G. Waxman. 1982. Rat optic nerve: freeze-fracture studies during development of myelinated axons. *Brain Res.* 250:1–20.

Blaugrund, E., S. Sharma, and M. Schwartz. 1992. L1 immunoreactivity in the developing fish visual system. *Brain Res.* 574:244–250.

Bloom, G. S., F. C. Luca, and R. B. Vallee. 1985. Microtubule associated-protein 1B: identification of a major component of the neuronal cytoskeleton. *Proc. Natl. Acad. Sci. USA.* 82:5404–5408.

Chen, Y., and J. Yang. 1971. A new approach to the calculation of secondary structures of globular proteins by optical rotatory dispersion and circular dichroism. *Biochem. Biophys. Res. Commun.* 44:1285–1291.

Chernoff, G. 1981. Shiverer: an autosomal recessive mutant mouse with myelin deficiency. *J. Hered.* 72:128.

Cohn, E. J., and J. T. Edsall. 1943. Proteins, amino acids, and peptides. Hafner Publishing Co. Inc. New York. 370–381.

Correas, I., J. Diaz-Nido, and J. Avila. 1992. Microtubule-associated protein tau is phosphorylated by protein kinase C on its tubulin binding domain. *J. Biol. Chem.* 267:15721–15728.

Davis, J., and V. Bennett. 1983. Brain spectrin—Isolation of subunits and formation of hybrids with erythrocyte spectrin subunits. *J. Biol. Chem.* 258:7757–7766.

Davis, J., and V. Bennett. 1984a. Brain ankyrin—a membrane associated protein with binding sites for spectrin, tubulin and the cytoplasmic domain of the erythrocyte anion channel. *J. Biol. Chem.* 259:13550–13559.

Davis, J. Q., and V. Bennett. 1984b. Brain ankyrin—purification of 72,000 Mr spectrin-binding domain. *J. Biol. Chem.* 259:1874–1881.

Davis, J., and V. Bennett. 1990a. The anion exchanger and Na/K ATPase interact with distinct sites on ankyrin in in vitro assays. *J. Biol. Chem.* 265:17252–17256.

Davis, L. H., and V. Bennett. 1990b. Mapping the binding sites of human erythrocyte ankyrin for the anion exchanger and spectrin. *J. Biol. Chem.* 265:10589–10596.

Davis, L. H., E. Otto, and V. Bennett. 1991. Specific 33-residue repeat(s) of erythrocyte ankyrin associate with the anion exchanger. *J. Biol. Chem.* 266:11163–11169.

Davis, J., T. McLaughlin, and V. Bennett. 1993. Ankyrin binding proteins related to nervous system cell adhesion molecules: candidates to provide transmembrane and intracellular connections in adult brain. *J. Cell Biol.* 121:121–133.

Diaz-Nido, J., L. Serrano, E. Meddez, and J. Avilia. 1988. A casein kinase II-related activity is involved in phosphorylation of microtubule-associated protein MAP1B during neuroblastoma cell differentiation. *J. Cell Biol.* 106:2057–2065.

Fellous, A., J. Francon, M. Lennon, and J. Nunez. 1977. Microtubule assembly in vitro: purification of assembly promoting factors. *Eur. J. Biochem.* 78:167–174.

Fischer, G., V. Kunemund, and M. Schachner. 1986. Neurite outgrowth patterns in cerebellar microexplant cultures are affected by antibodies to the cell surface glycoproteins L1. *J. Neurosci.* 6:605–612.

Goslin, K., D. Schreyer, J. H. P. Skene, and G. Banker. 1990. Changes in the distribution of GAP-43 during the development of neuronal polarity. *J. Neurosci.* 10:588–602.

Goslin, K., D. J. Schreyer, J. H. P. Skene, and G. Banker. 1988. Development of neuronal polarity: GAP-43 distinguishes axonal from dendritic growth cones. *Nature (Lond.).* 336:672–674.

Hall, T. G., and V. Bennett. 1987. Regulatory domains of erythrocyte ankyrin. *J. Biol. Chem.* 262:10537–10545.

Hisanaga, S., and N. Hirokawa. 1988. The structure of peripheral domains of the neurofilament revealed by low angle rotary shadowing. *J. Mol. Biol.* 202:297–306.

Hoshi, M., E. Nishida, M. Inagaki, Y. Gotoh, and H. Sakai. 1990. Activation of a serine/threonine kinase that phosphorylates microtubule-associated protein 1B in vitro by growth factors and phorbol esters in quiescent rat fibroblastic cells. *Eur. J. Biochem.* 193:513–519.

Inoue, Y., R. Nakamura, K. Mikoshiba, and Y. Tsukada. 1981. Fine structure of the central myelin sheath in the myelin deficient mutant Shiverer mouse,

with special reference to the pattern of myelin formation by oligodendroglia. *Brain Res.* 219:85–94.

Julien, J.-P., and W. E. Mushynki. 1982. Multiple phosphorylation sites in mammalian neurofilament polypeptides. *J. Biol. Chem.* 257:10467–10470.

Julien, J. P., and W. E. Mushynki. 1983. The distribution of phosphorylation sites among identified proteolytic fragments of mammalian neurofilaments. *J. Biol. Chem.* 258:4019–4025.

Kimura, M., H. Inoko, M. Katsuki, A. Ando, T. Sato, T. Hirose, H. Takashima, S. Inayama, H. Okano, K. Takamatsu, K. Mikoshiba, Y. Tsukada, and I. Watanabe. 1985. Molecular genetic analysis of myelin-deficient mice: Shiverer mutant mice show deletion in gene(s) coding for myelin basic protein. *J. Neurochem.* 44:692–696.

Kordeli, E., and V. Bennett. 1991. Distinct ankyrin isoforms at neuron cell bodies and node of Ranvier resolved using erythrocyte ankyrin-deficient mice. *J. Cell Biol.* 114:1243–1259.

Kordeli, E., J. Davis, B. Trapp, and V. Bennett. 1990. An isoform of ankyrin is localized at nodes of Ranvier in myelinated axons of central and peripheral nerves. *J. Cell Biol.* 110:1341–1352.

Kunimoto, M., E. Otto, and V. Bennett. 1991. A new 440-kD isoform is the major ankyrin in neonatal rat brain. *J. Cell Biol.* 115:1319–1331.

Martin, R., and B. Ames. 1961. A method for determining the sedimentation behavior of enzymes: application to protein mixtures. *J. Biol. Chem.* 236: 1372–1379.

Meiri, K. F., K. H. Pfenninger, and M. B. Willard. 1986. Growth-associated protein, GAP-43, a polypeptide that is induced when neurons extend axons, is a component of growth cones and corresponds to pp46, a major polypeptide of a subcellular fraction enriched in growth cones. *Proc. Natl. Acad. Sci. USA.* 83:3537–3541.

Michaely, P., and V. Bennett. 1993. The membrane-binding domain of ankyrin contains four independently-folded subdomains each comprised of six ankyrin repeats. *J. Biol. Chem.* In press.

Mikoshiba, K., K. Kohsaka, K. Takamatsu, and Y. Tsukada. 1981. Neurochemical and morphological studies on the myelin of peripheral nervous system from shiverer mutant mice: absence of basic proteins common to the central nervous system. *Brain Res.* 204:455.

Noble, M., S. A. Lewis, and N. J. Cowan. 1989. The microtubule binding domain of microtubule-associated protein MAP1B contains a repeated sequence motif unrelated to that of MAP2 and TAU. *J. Cell Biol.* 109: 3367–3376.

Otto, E., M. Kunimoto, T. McLaughlin, and V. Bennett. 1991. Isolation and characterization of cDNAs encoding human brain ankyrins reveal a family of alternatively spliced genes. *J. Cell Biol.* 114:241–253.

Pachter, L. S., and R. K. H. Liem. 1984. The differential appearance of neurofilament triplet polypeptides in the developing rat optic nerve. *Dev. Biol.* 103:200–210.

Rosenbluth, J. 1980. Central myelin in the mouse mutant Shiverer. *J. Comp. Neurol.* 194:639–648.

Sambrook, J., E. F. Fritsch, and T. Maniatis. 1989. Molecular Cloning: A Laboratory Manual. Cold Spring Harbor. Laboratory Press, Cold Spring Harbor, NY.

Sato-Yoshitake, R., Y. Shimura, H. Miyasaka, and N. Hirokawa. 1989. Microtubule-associated protein 1B: molecular structure, localization, and phosphorylation-dependent expression in developing neurons. *Neuron.* 3: 229–238.

Skoff, R. P., D. L. Price, and A. Stocks. 1976a. Electron microscopic autoradiographic studies of gliogenesis in rat optic nerve. I. Cell proliferation. *J. Comp. Neurol.* 169:291–313.

Skoff, R. P., D. L. Price, and A. Stocks. 1976b. Electron microscopic autoradiographic studies of gliogenesis in rat optic nerve. II. Cell Proliferation. *J. Comp. Neurol.* 169:313–334.

Srinivasan, Y., M. Lewallen, and K. Angelides. 1992. Mapping the binding site on ankyrin for the voltage-dependent sodium channel form brain. *J. Biol. Chem.* 267:7483–7489.

Sterberger, L. A., and N. H. Sternberger. 1983. Monoclonal antibodies distinguish phosphorylated and non-phosphorylated forms of neurofilaments in situ. *Proc. Natl. Acad. Sci. USA.* 80:6126–6130.

Tanford, C. 1961. Physical Chemistry of Macromolecules. John Wiley & Sons, Inc., New York.

Voter, W. A., and H. P. Erickson. 1982. Electron microscopy of MAP2. *J. Ultrastruct. Res.* 80:374–382.

Vulliet, P. R., F. L. Hall, J. P. Mitchell, and D. G. Hardie. 1989. *J. Biol. Chem.* 264:16292–16298.

Wang, D., S. A. Lewis, and N. J. Cowan. 1988. Complete sequence of cDNA encoding mouse MAP2. *Nucleic Acids Res.* 16:11369–11373.